RSC Advances

ROYAL SOCIETY OF CHEMISTRY

www.rsc.org/advances

RSC Advances

RSCPublishing

REVIEW

Simulations of Singlet Exciton Diffusion in Organic Semiconductors: A Review

Cite this: DOI: 10.1039/x0xx00000x

Josiah A. Bjorgaard,[a] Muhammet Erkan Köse [b,*]

Received 00th January 2014,
Accepted 00th January 2014

DOI: 10.1039/x0xx00000x

www.rsc.org/

This review describes exciton diffusion simulation strategies in condensed phase thin films of organic semiconductors. Methods for calculating energy transfer rate constants are discussed along with procedures for how to account for energetic disorder. Exciton diffusion can be modelled by using kinetic Monte-Carlo methods or master equations. Recent literature on simulation efforts for estimating exciton diffusion lengths of various conjugated polymers and small molecules are introduced. These studies are discussed in the context of the effects of morphology on exciton diffusion and the necessity of accurate treatment of disorder to accurately reproduce experimental results.

1. Introduction

Charge transport and energy transfer within conjugated organic semiconductors are fundamentally important properties of these materials for applications in organic electronics and sensors.[1] It has been unambiguously shown that both of these properties are strongly linked to crystallinity or long range order in films.[2-4] The morphology of such films determines the responses to current and optical pulses. While the dependence of charge mobility to crystallinity has been widely studied,[5] similar studies for energy migration are rather limited in the literature. In addition to morphology, the extent of energy transfer depends on the type of materials used for film fabrication. However, a comparative study to reveal structure-property relationships for energy transfer is still necessary.[3, 6, 7] The reason stems from the fact that it is rather difficult to separate the dependencies on morphological variations and structural variations in a single measurement method.

The electrically neutral excited state is composed of a bound electron-hole pair, which is referred as 'exciton'. The extent to which energy transfer causes excitons to migrate in

Dr. Josiah A. Bjorgaard received his bachelor's degree in Chemistry from Minnesota State University in 2010 and his PhD in Physical Chemistry at North Dakota State University in 2014 under the supervision of Assoc. Prof. Dr. Muhammet Erkan Kose. His doctoral studies spanned the fields of exciton diffusion length measurement and simulation. He currently holds a postdoctoral researcher position at the Center for Nonlinear Studies at Los Alamos National Laboratory, where his current research interests include quantum chemical solvation models, excited state molecular dynamics, and nonlinear optical properties.

Assoc. Prof. Dr. Muhammet Erkan Köse got his bachelor's and master's degree in Chemistry at Bilkent University, Ankara, Turkey in 2001. He received his PhD degree at the chemistry department of University of Florida in 2005. After spending four years at Clemson University (South Carolina, USA) and National Renewable Energy Laboratory (Colorado, USA) as postdoctoral researcher, he moved on to become a faculty member at the Chemistry and Biochemistry department at North Dakota State University (North Dakota, USA). In 2012, Prof. Köse moved to Turkey and was appointed as Senior Head Researcher at TUBITAK, Gebze campus. In his career, Prof. Köse published both theoretical and experimental work to better understand material properties geared towards specific applications. Currently, his research interests include energy transfer measurements/simulations in organic semiconductors, organic photovoltaic devices, organic light emitting diodes, and flexible transparent electrodes.

the bulk medium is exemplified by the magnitude of exciton diffusion length (L_D). Exciton diffusion has important implications in a wide range of important electronic devices.[8] For instance, it is of high significance to exploit conjugated materials with large L_Ds to be used in organic solar cells. Longer exciton diffusion distances ensure that the exciton can find an acceptor before radiative or non-radiative decay and decreases the dependence of current generation efficiency on donor/acceptor blend morphology. In contrast, short L_Ds are preferred for the active layer of organic light emitting devices to suppress exciton-exciton annihilation and other decay mechanisms.

There are many methods to measure L_D in conjugated organic semiconductors. Although L_D plays a key role in efficient operation of organic solar cells, the correlations between molecular structure, morphology, and L_D is not well established and remains a current area of research. One of the reasons for the lack of such understanding is inconsistent L_D results reported even for the same polymer. For instance, a widely studied conjugated polymer in organic solar cells, poly(3-hexylthiophene) (P3HT), is reported to have L_Ds ranging from 2.6 to 27 nm (Table 1). Similar variation can be also noticed for poly(2-methoxy-5-(2′ethyl-hexoxy)-1,4-phenylene-vinylene) (MEH-PPV). Such conflicting reports are mostly caused by differing chemical sample (different molecular weights, regioregularity, purity, etc.), measurement method, and inadequate modelling of generated data. It is therefore vital to conduct measurements on various materials under the same conditions in order to extract meaningful data for comparison. Such studies are absolutely necessary to understand how conjugation length, structural rigidity, functional group, crystallinity, crystal phases, and molecular weight affect L_D in this important class of materials. Such an understanding could help rational design of novel conjugated materials for specific device and sensor applications. The reported L_Ds for conjugated polymers and small molecules show significant differences (see Table 1), with the latter having larger numbers. This is probably caused by higher tendency of small molecules to adopt crystalline structures in solid state,[3] hence promoting excitons to diffuse longer distances.

Since there are many factors that could affect the magnitude of L_D, theoretical simulations of exciton diffusion can help to explain the experimental observations and shed light into factors important for exciton migration in conjugated materials. Indeed, some recent literature reports reveal the important parameters for exciton diffusion with the help of multi-scale modelling studies.[9] Validated simulation methodologies could serve as an alternative to time-consuming experimental measurements of L_D. In addition, simulations can provide deeper understanding of energy transfer mechanisms at microscopic scale, which are not accessible by experiment. Further, the variations in material structure, morphology, and purity can be controlled by performing appropriate changes in the simulation codes.

This review is intended to summarize the latest advances in the field of exciton diffusion simulations in organic semiconductors. There is a vast literature on energy transfer processes for π-conjugated systems.[1, 10] Here, we narrow our overview to the materials and processes mostly relevant to L_D studies. It is not our goal to present a comprehensive review on the topic, but summarize the latest important work, discuss main approaches to simulate L_D, and compare theoretical results with experimental ones if applicable.

Simulation of L_D frequently requires many theoretical methods and approaches to be used sequentially in a multistep procedure. Each method/step should be carried out carefully in order to achieve meaningful results. This review is structured as follows: The first section discusses the nature of excitons assumed in diffusion simulations. The framework for simulation studies is presented in the following section where rate constants, energetic disorder, and modelling techniques are introduced. The last chapter focuses on how morphology of simulated film affects the magnitude of L_D and importance of trap sites for accurate simulation studies. The review is concluded with a discussion of the usefulness of exciton diffusion simulations and outlook.

Table 1 Measured exciton diffusion lengths of selected conjugated materials and small molecules.

Polymer/Quencher (Exp. Details)	L_D (nm)	Reference
P3HT/TiO_2 (92% RR)	2.6 - 5.3	Kroeze[11]
P3HT/TiO_2 (98.5% RR)	8.5 ± 0.7	Shaw[12]
P3HT/None (98.5% RR)	27 ± 12	Cook[13]
P3HT/HOPG (93% RR)	8 ± 2	Köse[6]
P3HT/PCBM (blend)	5.4 ± 0.7	Mikhnenko[14]
MEH-PPV/C_{60} (cross-linked)	6.3	Markov[15]
MEH-PPV/None (TR PL)	5 - 8	Lewis[16]
MEH-PPV/Quencher Dyes (RET)	4.5 ± 0.5	Bjorgaard[17]
MEH-PPV/None (single chain, hole injection device)	13.7	Bolinger[18]
NRS-PPV/C_{60} (cross-linked)	5 ± 1	Markov[19]
MDMO-PPV/TiO_2	6 ± 1	Scully[20]
BEH-PPV/C_{60} (cross-linked)	6	Markov[15]
LPPP/C_{60} derivative (blended)	6	Haugeneder[21]
C–PCPDTBT and Si–PCPDTBT/PCBM (blend)	10.5 ± 1	Mikhnenko[14]
TFB/PCBM Derivatives (TR PL)	9 ± 2	Bruno[22]
Small Molecule/Quencher (Exp. Details)		
PTCDA/C_{60} (varying crystallinity)	6.5 – 21.5	Lunt[3]
TnBuPP/TiO_2	22 ± 3	Huijser[23]
Alq3 (amorphous film, device meas.)	10-30	Garbuzov[24]
C_{60} (device meas.)	30 - 35	Qin[25]
Pentacene (device meas.)	65 ± 16	Yoo[26]
Conjugated dendrimers/HOPG	8 – 17	Köse[6]
di-indeno-perylene/CuPc	60	Topczak[27]

RR: Regioregular, HOPG: Highly ordered pyrolytic graphite, MDMO-PPV: poly[2-methoxy-5-(3’,7’-dimethyloctyloxy)-1,4-phenylenevinylene], NRS-PPV: poly[{2-(4-(3’,7’-dimethyloctyloxyphenyl))} -co{2-methoxy-5-(3’,7’-dimethyloctyloxy)}-1,4-phenylenevinylene], BEH-PPV: poly(2,5-bis(2′-ethyl-hexyl)–1,4-phenylenevinylene), LPPP: ladder-type poly(para-phenylene), C–PCPDTBT: poly[2,6-(4,4bis-(2-ethylhexyl)-4H-cyclopenta[2,1-b;3,4b’]dithiophene)-alt-4,7-(2,1,3-benzothiadiazole)], Si–PCPDTBT: poly[(4,4’-bis(2-ethylhexyl)dithieno[3,2-b:2’,3’-d]silole)-2,6-diyl-alt-(2,1,3-benzothiadiazole)-4,7-diyl], TFP: poly [9,9-dioctylfluorene-co-N-(4-butylphenyl)-diphenylamine], PTCDA: 3,4,9,10-perylene tetracarboxylic dianhydride, TnBuPP: meso-tetra(4-n-butylphenyl)porphyrin, CuPc: Copper(II) phthalocyanine, Alq3: Tris (8-hydroxyquinoline)aluminum, RET: Resonance energy transfer, TR PL: Time-resolved photoluminescence spectroscopy

2. Modelling Exciton Transport

2.1 Near Band gap Singlet Excitons in Organic Semiconductors

The predominant number of published exciton diffusion simulations in bulk organic semiconductors are performed for singlet excitons, thus we restrict the review to these species. This is not meant to say that measurements/simulations have not been performed for triplet excitons, nor that they are insignificant for optoelectronic applications, but simply to limit the topic of this review to the major component of the literature. Near band gap singlet excitons in organic semiconductors are generally considered to be purely Frenkel in nature with exciton binding energy significantly larger than kT.[28] These excitons are assumed to be localized on single molecules or single polymer chains. In conjugated polymers, they are thought to exist at certain sections of the chain. This is mostly a result of torsional disorder (Fig. 1), which causes disruptions in π-orbital conjugation.[29-31]

The simulation methods presented in this review are applicable to the diffusion of localized singlet excitons. The usefulness of localization is that one can build a bulk simulation strategy from calculations performed on single molecule/polymer chains. Rate constants for energy transfer between bimolecular complexes can then be used to calculate bulk diffusion properties. A further requirement is that the relaxation of excitons after hopping is rapid. This makes the transport a Markovian process, i.e. the probability of the next transport event does not depend on the previous transport event. If the localization of the exciton is dynamic and happens on the time scale of the transport process or the exciton is delocalized extensively such that isolated chromophoric subunits of the bulk cannot be determined, many of the simulation procedures reviewed here would require modification.

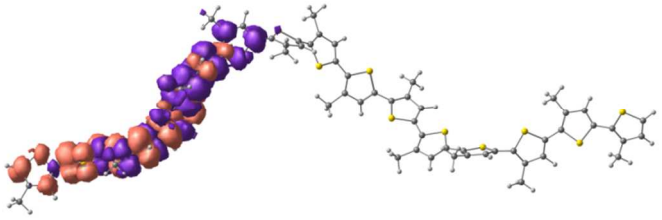

Fig. 1 Localization of an exciton in an oligo(3-methylthiophene) chromophore due to torsional disorder.

The single chain or single molecule nature of these excitons is an approximation and in many cases its validity can be argued.[32] Nonetheless, an example using the prototypical conjugated polymer P3HT shows that exciton localization is a reasonable approximation. This was shown by Paquin et al.[33] using an H- and J-aggregate model of polymer chains in ordered conformations (Fig. 2). They calculated an exciton coherence function which showed, by the magnitude of the coefficients shown in Fig. 2, how localization of the exciton occurs in -stacked polymer chains. The exciton is not localized on a single chain in their model, but predicted to be delocalized over approximately two chains. This represents a completely ordered case, but typical organic semiconductors in device structures possess a disordered morphology. Exciton delocalization has been shown to decrease with static energetic disorder.[34] Considering both ordered and disordered phases, it can be argued that the single chain/single molecule regime is appropriate for most of the conjugated materials, especially for those with intrinsic disorder.

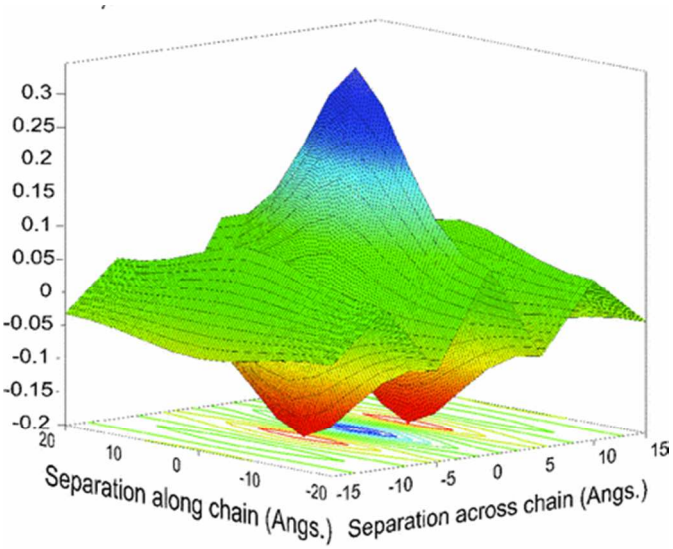

Fig. 2 Simulation of exciton coherence in a crystalline aggregate of P3HT chains, showing localization across chains and along the chains. The exciton shows significant coherence across approximately 3 chains, though the coefficients are largest in magnitude on single chain. Adapted from Paquin, F. et al., Phys. Rev. B, 88, 155202, 2013. Copyright 2013 by the American Physical Society.[33]

Exciton confinement provides an explanation for reduced excited state energy in planar π-systems and is in agreement with the increased absorption maximum in oligomers of increasing length.[35] This is not always the case for disordered systems with torsional degrees of freedom between conjugated segments, where the excitation energy can be coupled to the internal disorder of the conjugated system. These segments are separated into chromophores by severe torsional defects, thus, at least for the lowest energy excitons, polymer chains can be viewed as a chain of separated chromophores.[29, 36] Exciton localization and energetic disorder have important implications in exciton diffusion processes in conjugated materials.

The relaxation of the nuclear structure of chromophores due to exciton confinement can also be significant. The effects of nuclear relaxation on exciton diffusion have been addressed in recent years.[37, 38] Nuclear relaxation causes 'hot' excitons to lose energy and form thermally relaxed 'cold' excitons. In extended systems, such as in conjugated polymers, this has been predicted to lead to localization or reduction in exciton size because of vibrational relaxation. The influence of the exciton localization process on the energy transfer rates can also be significant, which will be discussed below.[39]

In order to fullfill the Markovian condition described above, the following criteria should be satisfied. The coupling must be

significantly weak so that the hopping rate is slow enough to allow full thermalization of the chromophore, hence allowing formation of cold excitons. Thus, the relaxation energy is not used to surpass the hopping barrier for other sites. If the coupling between sites is strong enough and thermalization of excitons does not occur rapidly, then ballistic and coherent transport dynamics can occur. This may be the case for hot excitons.[40-42] It is necessary to have weak enough electronic coupling between chromophores in order to avoid the effects of strong coupling regime if one is to describe exciton migration as diffusion and calculate rates as described in the following section.

2.2 Energy transfer rates

Here, we discuss the methods and approximations that have appeared in the recent literature of singlet exciton diffusion simulations (Fig. 3). Descriptions of other types of energy transfer mechanisms such as Dexter energy transfer, which can be observed in exciton transport[1, 8] and specifically in the separation of long and short range effects, can be found elsewhere.[10, 43] The basis for exciton diffusion simulations is the golden rule, given by

$$\Gamma_{nm} = \frac{2\pi}{\hbar}|V_{nm}|^2 D_{nm} \quad (1)$$

where V_{nm} is the matrix element between states n and m given by $\langle n|H'|m\rangle$. D_{nm} is the joint density of states when describing hopping from an ensemble to a manifold of states or alternatively is the final density of states when describing hopping from one state to a final manifold of states. The initial state n is an eigenfunction of the zeroth order Hamiltonian H_0 and the perturbation H' gives the matrix element coupling the two states. Hopping rates are in general given by approximating the parameters of the golden rule. A few approximations yield to Eq. 1, which is the solution of the coupled two-level system to first order in the state coupling perturbation of magnitude, V_{nm}. First, it is assumed that this perturbation is sufficiently weak to not perturb the eigenstates of the system. This is called the weak coupling regime and it allows one to perform calculations on isolated chromophores. Second, the time scale of the interaction is assumed to be very long compared with the period of the quantum mechanical oscillatory interaction of the two molecules. This is related to the thermalization condition such that dephasing occurs. The result of the second condition is energy conservation, since the hopping process is assumed to occur instantaneously.

Both experiment and theory give support for this incoherent transport phenomenon, since relaxation rates are determined to be much faster than occupation times.[44, 45] The experimental evidence shows significant energy relaxation upon photoexcitation, exemplified by large Stoke's shifts occurring in less than 200 fs in conjugated polymers and oligomers.[46, 47] Therefore, the absorption and emission spectra can be used to approximate the joint density of states.[48, 49]

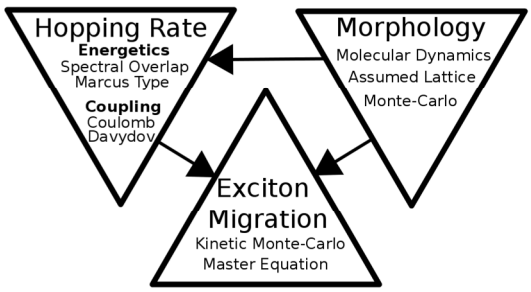

Fig. 3 Schematic of methods used for exciton migration simulation described in this review and their interrelation. Initially, bulk morphology is simulated or assumed and then hopping rates are determined, followed by simulation of exciton migration, which also draws information from the simulated bulk morphology.

When the combined density of states is determined from the absorption and emission spectra of an ensemble of chromophores, the golden rule is written as

$$k_{nm} = \frac{2\pi}{\hbar}|V_{nm}|^2 J_{nm} \quad (2)$$

where J_{nm} is the spectral overlap integral for an ensemble of molecules and given by

$$J_{nm} = \int_0^\infty f_m(\lambda)\varepsilon_n(\lambda)\lambda^4 d\lambda \quad (3)$$

The term, $f_m(\lambda)$, is the dimensionless emission spectrum of the donor and $\varepsilon_n(\lambda)$ is the extinction coefficient of the acceptor at the wavelength λ. This is related to the ensemble average of a simple energy conservation condition. Further variations on this term have been derived when considering thermally assisted transport and coupling to vibrational modes.[50] Eq. 3 has found wide application areas in experimental fields for determining energy transfer rates of the Förster type. The basic use of Eq. 3 requires that one determines the rate for an ensemble of initial and final states, such as those found in the steady state optical spectrum of solvated chromophores. The spectral overlap integral has been used extensively in exciton diffusion simulations.[6, 45]

The hopping rate in many exciton diffusion simulations does not correspond to the ensemble average, since the hopping rate is calculated for hopping from one local site to several nearby sites, which may have some local order. Then, Eq. 3 can only find accurate use when applied to homogeneous materials, so that the result is an averaged diffusion length. Correlation between spatial and energetic disorder in inhomogeneous materials prevents the accurate use of Eq. 3.

There are a number of methods for calculating the excitonic coupling integrals between chromophores.[51, 52] For a heterodimer of coupled two-level molecules, $|J_{nm}|$ from Eq. 2 is given from first-order perturbation theory of a two level system by

$$V_{nm} = \frac{1}{2}\sqrt{(E_+ - E_-)^2 - (E_n - E_m)^2} \quad (4)$$

where E_+/E_- are the upper/lower excitation energies of the coupled dimer system and E_n/E_m are the uncoupled excitation energies. For systems with no degeneracy, this gives the coupling matrix element for the golden rule. In general, one must calculate both the coupled and uncoupled excitation energies to determine V_{nm}. For a homodimer, this equation simplifies to half of the excitation energy splitting in the coupled system.[53] This approach is related to the well-known Davydov splitting.[54] There is no mistake that Davydov splitting blends well with the idea of electronic coupling in the golden rule since it is also the result of the first order perturbation of a coupled two level system. The advantage of this approach is that, depending on the *ab initio* method chosen to calculate the excited states, it can include exchange and higher order correlation terms as opposed to other methods, which consider only Coulombic coupling. The process of expanding the coupling of this form into Coulomb, exchange, and higher order terms has been extensively surveyed elsewhere.[10, 45, 55, 56]

A 'supermolecular' calculation, i.e. a quantum chemical treatment of a coupled bimolecular complex, is potentially computationally expensive. However, the calculation of supermolecular excited state or excitation energies for a full bimolecular system is an accurate means of determining the coupling integrals for chromophores in close proximity. Of course, this is dependent on the ability of the first principles method to accurately capture dispersive and long-range interactions.[57] Nonetheless, most methods accurately capture the contribution from Coulombic coupling, which is the major factor in determining the magnitude of the electronic coupling integrals. Although the bimolecular calculation is of higher cost, this has recently been performed with separation of the dimer into subsystems. This approach significantly reduced the computational cost for a time dependent density functional theory (TD-DFT) framework.[58]

For large oligomers and polymers, the computational cost required for a TD-DFT calculation on dimers may be quite high, especially when calculations are conducted on many bimolecular complexes as in the case of disordered materials. More frequently the electronic coupling is given using the Coulomb interaction between transition densities, (ρ_n), which describes the transitions between the ground and excited states. This approach neglects exchange and higher order correlation terms and captures only Coulombic coupling.[10, 45, 59] This relevant coupling integral is expressed as

$$V_{nm} = \int_{R^3} \frac{\rho_n(r)\rho_m(r')}{|r-r'|} dr dr' \quad (5)$$

Transition densities are generally calculated from single reference *ab-initio* methods such as TD-DFT.[60, 61] Eq. 5 can be rearranged into a form including Poisson equation.[6] The resulting equation can be solved with any efficient Poisson solver,[62] yielding Coulombic coupling integrals between chromophores without significant computational cost. The use of a discretized set of points to represent transition density in Eq. 5 is referred to as the transition density cube (TDC) method.[63] In the Tamm-Dancoff approximation,[61] the transition density is given by

$$\rho_n(r) = \sum_{\mu\nu} c_{\mu\nu}^{(n)} \phi_\upsilon(r)\, \phi_\mu(r) \quad (6)$$

where $\phi_{\mu,\upsilon}(r)$correspond to the occupied (μ) and unoccupied (ν) orbitals and $c_{\mu\nu}^{(n)}$ are the coefficients resulting from the configuration interaction (CI) expansion coefficients of electronic transition from ground state to the excited state *n*.

The electronic coupling integral is most easily evaluated within a point dipole approximation (PDA) to describe the energy transfer based on Förster mechanism.[10] V_{nm} in the PDA is described as,

$$\mathrm{V}_{nm} = \frac{\mu_n\mu_m}{r^2}(\cos(\theta) - 2\sin(\theta)) \quad (7)$$

where μ is the transition dipole, *r* is the distance between centers of charge for the transition densities and θ is the angle between transition dipoles. Utilizing Eq. 7 in Eq. 2 gives the Förster theory rate expression for exciton transfer.[64, 65] This can be used to describe long range exciton transfer beyond nearest neighbour hopping. However, Eq. 7 fails at short distances to describe accurate rates because of the neglect of higher order multipole terms in the Coulombic interaction, as well as the neglect of all exchange and correlation effects.[51] Despite its inadequacy, it has been widely applied in the literature.[10]

For conjugated polymers and small molecules with repeat units, modifications have been proposed to the PDA such as the line dipole approximation[66, 67] and the improved Förster model.[45] The line dipole approximation partially takes into account chemical structure and topology by partitioning the molecule into subunits and defining local transition dipoles. It has successfully been used to describe the experimental anisotropy decay in solvated polymer segments.[68] Similarly, the improved Förster model is calculated from an independent neglect of differential overlap (INDO) scheme so that the electronic coupling is the sum of pairwise interactions between each pair of donor and acceptor atoms, making coupling calculations with this method very fast.

2.3 Energetic Disorder and Uphill Transport

The effects of disorder on carrier and exciton diffusion were studied in the 1970's and 1980's using analytical and Monte-Carlo studies.[69-74] These studies were performed on ordered lattices, frequently assuming Boltzmann populations for the exciton energy distribution. A recent study[75] shows that the early methodologies are inadequate to describe experimental exciton diffusion lengths. For better correspondence with the experimental results, it was shown that it is necessary to use the broadened energetic distributions and a spatially disordered lattice when describing realistic disordered systems.[75] Many studies reviewed in the following sections have used these essential aspects and found good correspondence with the experiment.

Recent approaches have utilized a different definition of the joint density of states than that of the Förster model. Using a

Marcus type rate equation,[9, 76] the exciton diffusion rate constant is obtained by using reorganization energies. This eliminates the need to use the inhomogeneously broadened bulk spectra. Inhomogeneous broadening involves the broadening of spectral lineshapes due to varied internal and external conformations of chromophores.[77] Here, the inhomogeneous broadening specifically refers to the broadened absorption and emission spectra by including the coupling effects from larger transition dipole moments (effectively seen as variation in oscillator strength in the optical spectra) and energetic effects from broadened energy distributions.

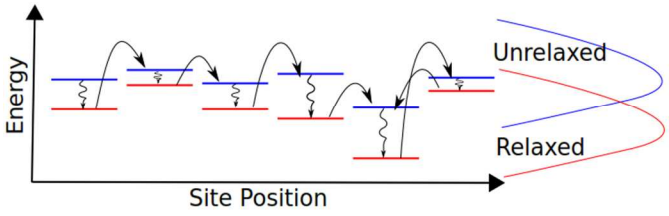

Fig. 4 Schematic of exciton diffusion with energetic disorder such that trapping can occur. Comparison between site energies and inhomogeneously broadened distributions is given for relaxed and unrelaxed geometries. The arrows show a possible trajectory with hops from the relaxed exciton to unrelaxed exciton with nonradiative relaxation upon site occupation. The final reverse hop demonstrates how low energy sites can cause trapping to occur by increasing the hopping rate to the low energy trap site.

In a homogeneously disordered system where each hopping rate is calculated with parameters derived from the same distributions, an average diffusion length can be easily calculated using ensemble average properties. This is correct as long as the disordered properties are delta correlated so that they can be considered as having independent distributions. For example, there should be no correlation between interchromophore distance and energy difference between two sites. For systems with varying nanoscale morphologies like in many semicrystalline polymers, disorder has to be considered explicitly because of the interplay between ordered and disordered regions.[9] Only then can morphological effects on exciton diffusion be given correctly in order to account for the effects of inhomogeneous broadening associated with various intermolecular conformations. In a study by Papadopoulos et al., the difference in L_D between the disordered and the liquid crystalline phases of an indenofluorene oligomer is negligible due to fortuitous cancelling of the electronic coupling and spectral overlap terms in Eq. 1.[78] Still, this is not likely to be the case for most systems.

When disorder is presented explicitly in the form of site energy disorder (Fig. 4), a proper description of transport requires consideration of thermal hopping, i.e. phonon assisted transport. Thermal hopping involves excitonic coupling to vibrational modes for hopping to states with large energy barriers. The simplest and most commonly used model of thermal hopping is given in the form of Miller-Abrahams (MA) hopping rate (Eq. 8). This formalism is widely used for charge transport simulations in disordered media[5] and describes the coupling to a classical Boltzmann distributed phonon bath. The MA hopping rate is given by

$$\tilde{k}_{nm} = k_{nm}\begin{cases} e^{(E_n - E_m)/kT}, & \text{for } E_m > E_n \\ 1, & \text{for } E_m \leq E_n \end{cases} \quad (8)$$

When the energy is decreased by a hop, the MA rate is equivalent to $\boldsymbol{k_{nm}}$. Hops which are upwards in energy can occur by drawing energy from the Boltzmann distributed phonon bath.

2.4 Accuracy of Calculated Rates

We now turn to the important aspects of calculating accurate parameters for transition rates to best represent energy transfer for exciton diffusion. The comparison of the magnitude of the calculated parameters with experiment is difficult. For example, one might determine V_{nm} from experiment through either the distance dependence of long range energy transfer or from the splittings in aggregates according to Eqs. 7 and 4, respectively. Since the distance dependence of energy transfer rates does not give the full information about the couplings for closely packed chromophores because of higher order multipole effects, one must resort to aggregate models to better simulate short range energy transfer.[32, 79-81] The parameters for comparison to aggregate models, e.g. Davydov splittings, are difficult to extract from experiment since the splittings are in general too small to determine from bulk measurements.

Quantum chemical methods are generally used for calculating V_{nm}.[6, 39, 63] Frequently, the INDO approximation with a single excitation configuration interaction (INDO/CIS) has been used for calculation of transition density or transition dipole couplings.[44] TD-DFT methods have also been used for similar simulations.[7, 9]

Both TD-DFT and INDO/CIS methods seem to have good correspondence with experimental transition energies for monomeric systems. The rate calculated with golden rule (Eq. 1) can be approximately related to the transition dipole from Eq. 7. In this case, the deviation in the transition dipole moment, if large, can result in a significant error in the hopping rate. Thus, it is important to choose methods which predict accurate transition dipole moments when estimating the magnitude of electronic coupling integrals.

Organic semiconductors generally have significant excited state reorganization energy. It is necessary to calculate the coupling between a local exciton ground state (LEGS) and vibrationally relaxed state (VRS). These terms were recently coined by Tozer and Barford but the initial idea that vibrational relaxation would have a significant impact on the electronic coupling was mentioned by Beljonne et al. several years before.[44, 45] A VRS is the result of the shift in exciton energy and structure (cold exciton) upon relaxation on the excited state potential energy surface, while the initial excited state relaxation on the ground state potential energy surface is a LEGS.[37, 38, 39, 82]

In exciton migration, the electronic coupling occurs between a VRS and a LEGS. In practice, this involves

calculation of the electronic coupling of a molecule in the optimized ground state geometry with a molecule in the optimized excited state geometry. The general idea that the relaxed state was necessary to calculate electronic coupling was expanded in order to include the necessary localization effects upon relaxation.[38, 82] The result is some dynamic localization such that the relaxation process results in transport (Fig. 5). Dynamic localization was shown to have a significant effect for MEH-PPV polymer, yet it has not been included in other simulations to date and a recent publication by the authors suggested that the contribution of VRS to exciton migration is instead negligible.[83]

An important question that has been posed when examining exciton transport is the difference between intra- and interchain transport rates in conjugated polymers. Differing viewpoints have been given in the literature.[44, 45, 51] The variation in inter- and intrachain coupling integrals has been extensively studied by Beljonne et al. for polyindenofluorene endcapped with

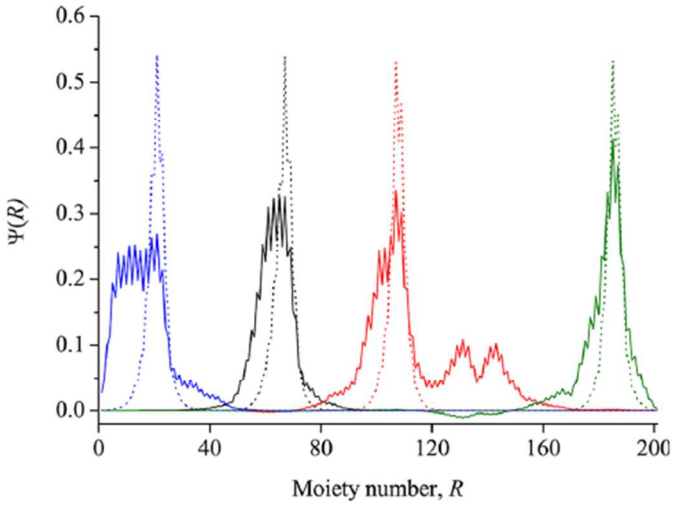

Fig. 5 Calculations of local exciton ground states (solid) and vibrationally relaxed states (dotted) show dynamic localization of excitons on a poly(p-phenylenevinylene) chain. Reprinted with permission from O. R. Tozer, E. Bittner and W. Barford, J. Phys. Chem. A, 2012, 116, 10319. Copyright 2012 American Chemical Society.[82]

perylene derivatives[44] and Köse for oligothiophenes.[51] Exciton migration has been revealed to critically depend on the arrangement of chromophores in inter- or intrachain morphologies using a Förster type rate equation. The spatial arrangement and size of interchain segments were shown to have a drastic impact on the electronic coupling integrals.[45] The relevant study by Hennebicq et al. suggested that interchain transport is the major pathway for exciton migration at thermal equilibrium but there is no major consensus in the literature on which pathway is most important for exciton diffusion.

3. From Energy Transfer to Energy Migration

3.1 Kinetic Monte-Carlo Algorithms

Once appropriate methods are utilized for calculating excitonic coupling integrals and joint density of states, it is then rather straightforward to estimate the energy transfer rate constant for the system of interest. A kinetic Monte-Carlo scheme is generally used for random walk simulations in many different situations to estimate the L_D in organic semiconductors.[84, 85] To do so, we first consider the set of all rates, Q_m, for processes which are associated with an active site on a given lattice to deactivate the site, e.g. the transfer or an exciton at site m to site $n = 0,1, \dots, N$,

$$Q_m \coloneqq \{k_{0m}, k_{1m}, \dots, k_{Nm}\} \quad (9)$$

and the sum of these rates

$$\sum_n k_{nm} = R_m \quad (10)$$

Standard kinetic Monte-Carlo schemes consider a choice of a path by choosing a random number u such that uR_m falls within the bounds of one of the rates in a cumulative sum of the set Q_m. Then, it follows from first order kinetic theory that the residence time at site m can be calculated as

$$t_m = -(log v)/R_m \quad (11)$$

where υ is a second random number. At each step, new rates Q_m are calculated for a given site. The parameters which were used to calculate the rate selected by u from a given step are saved and used to determine the next set of rates.

This process is repeated and the trajectory of the occupied site is followed over the course of many samples. For example, 10,000 trajectories might be followed over 1,000 subsequent hops to give a meaningful average property related to the site residence time or trajectory length. In contrast, one might also use the photoluminescence lifetime to end a trajectory in the simulation algorithm.[6]

To examine properties such as maximum distance travelled, the trajectories can be binned to form a histogram plot (Fig. 6). The diffusion length is the experimental property of interest, which is extracted from the histogram plot. One can also calculate the diffusion coefficient, D, by using the experimental fluorescence lifetime (τ) and the following well-known relation

$$D = \sqrt{2dL_D\tau} \quad (12)$$

where d is the dimensionality of the diffusion process.

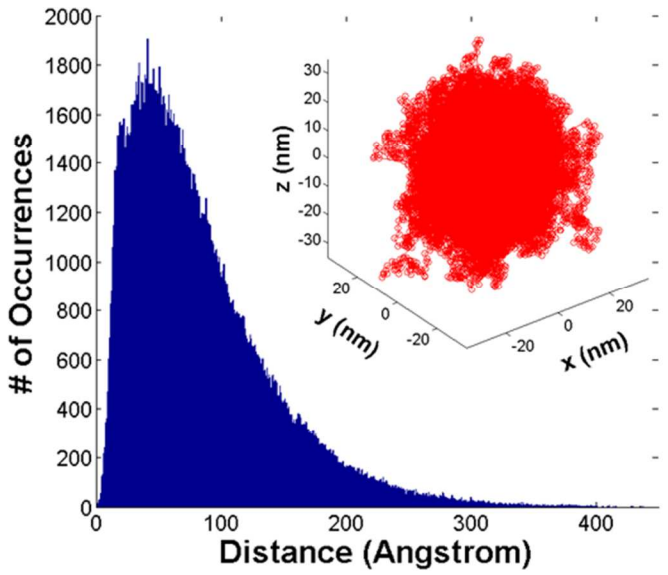

Fig. 6 Kinetic Monte-Carlo simulation of exciton hopping trajectories and histogram binning of exciton migration distances. The inset shows how exciton quasiparticle migrates in 3D space starting from (0,0,0) position. Reprinted with permission from Kose et al., Chem. Phys. Chem., 2009, 10, 3285-3294. Copyright 2009 John Wiley & Sons Inc.[6]

3.2 Master Equation

Exciton transfer simulations can be performed with master equations as well.[45, 48] A master equation is a set of first-order differential equations describing the time evolution of occupation probability of a system to occupy each discrete set of states with respect to variable t. The master equations' central quantity is P_n, which expresses the probability of an exciton occupying site n at time t.

$$dP_n/dt = \sum_m k_{mn}P_m - k_{nm}P_n \quad (13)$$

The above equation is simplified version of actual master equation where the terms with $m = n$ do not appear in the summation. The magnitude of occupation probability, P_n, depends on the contribution from all other states to n. Eq. 13 is especially useful for crystalline lattices without disorder, since the equations are solvable analytically due to translational symmetry. This results in hopping probabilities in each lattice direction. Using this method, the hopping rates can be converted to diffusion lengths quite readily.

4. Simulations

4.1 Morphologies

Both simulations and experiments have shown strong influences of condensed phase morphology on exciton diffusion length.[86] These morphologies can be crystalline, semicrystalline, or totally disordered in nature.[4, 87, 88] For example, experimental studies using spectrally resolved photoluminescence quenching[3] and exciton annihilation rates in semicrystalline polymer films have shown that the crystallinity has a strong influence on the magnitude of exciton diffusion length (Fig. 7) and the diffusion can be anisotropic in crystalline domains.[89, 90] One dimensional exciton diffusion length in crystalline P3HT domains has been found as 20 nm, which is larger than the bulk value.[89]

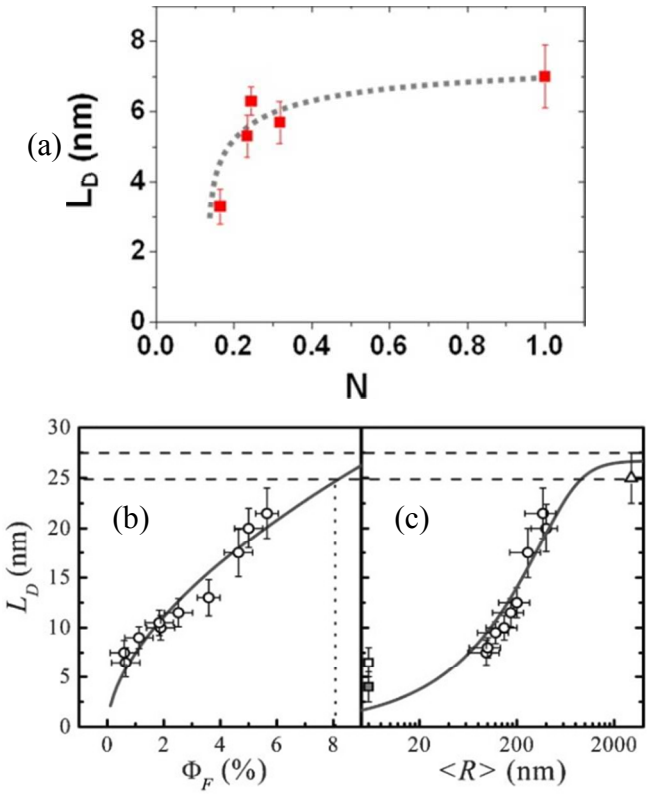

Fig. 7 (a) Experimentally determined exciton diffusion length as a function of crystallinity parameter N for P3HT. Reprinted with permission from M. Sim et al. J. Phys. Chem. C. 2014, 118, 760-766. Copyright 2014 American Chemical Society.[90] (b) Variation in measured L_D with fluorescence quantum yield and (c) mean crystal diameter in PTCDA films. The single crystalline limit is indicated by dashed lines. L_D changes as a function of grain size due to non-radiative quenching at grain boundaries. Adapted with permission from R. R. Lunt, J. B. Benziger, and S. R. Forrest, Advanced Materials, 2010, 22, 1233-1236. Copyright 2010 John Wiley & Sons Inc.[3]

A similar behavior was noticed long ago for triplet exciton diffusion in anthracene crystals.[91] For perfectly ordered materials, the calculation of exciton diffusion length is simple since there are a small number of rates for well-defined directions. If the energetic disorder is negligible, the final density of states is a Dirac delta function at the LEGS energy. Then, Eq. 13 can be diagonalized analytically to yield transport rates which, when combined with the exciton lifetime, yields one-dimensional diffusion lengths in the material. Similarly, the anisotropy of electronic couplings[51] and singlet exciton diffusion[92] in organic semiconductor crystals has been predicted from *ab initio* methods. Such observations are important for device applications, since it may cause diffusion to be one-dimensional depending on the crystalline packing morphology.

The crystalline structure of conjugated polymers can be lamellar.[87, 88] Joint experimental and theoretical studies have

been performed to investigate the impact of lamellar structure on exciton diffusion.[93] Hopping rates are calculated between lamellae with inclusion of energetic disorder and qualitative results show that excitons become trapped at low energy sites as lamella becomes smaller. This suggests that higher molecular weight polymers can be used to increase the exciton diffusion length by reducing trapping.[93] Trapping of excitons has severe consequences for amorphous materials as discussed below.

The interplay between ordered and disordered domains is known to affect charge transport properties,[4] therefore it is no surprise that there are similar implications on exciton transport properties of materials as well. Recent simulations of trapping and exciton diffusion in semicrystalline P3HT have shown that trapping occurs in crystallites, not at a single site but within a group of sites with crystalline order. The exciton is then unable to migrate significant distances in the surrounding amorphous phase (Fig. 8).[9] The one dimensional L_D in crystalline and amorphous P3HT domains has been simulated as ~20 nm and 5.7 nm, respectively.[9] These numbers agree very well with the reported experimental L_Ds listed in Table 1.

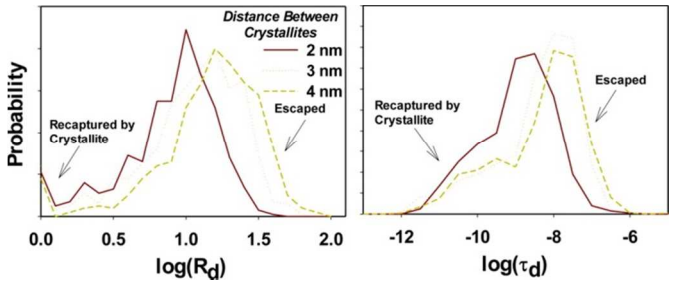

Fig. 8 Probability of maximum distance travelled (R_d) and site occupation time (τ_d) for excitons hopping in amorphous material around crystallites that are simulated using Monte-Carlo techniques with inclusion of energetic disorder. Trapping occurs in the crystallites as shown by the ratio of recaptured to escaped site occupation times. Reprinted with permission from J. Bjorgaard and M. E. Kose, J. Phys. Chem. C, 2014, 118, 5756-5761. Copyright 2014 American Chemical Society.[9]

Studies without appropriately described disorder in the rate parameters seem to overestimate experimental L_Ds. This can be seen by comparing studies that have focused on the effects of amount and type of disorder in semiconducting organic thin films. A series of studies by Athanasopoulos et al. included disorder in different terms in the golden rule rate expression.[94-96] These studies were performed for different conjugated polymers, yet they showed drastically different results compared to those of experiments. The initial study overestimated exciton diffusion length by an order of magnitude when disorder was included in the electronic coupling calculations with the transition density cube method.[96] In this study, the polymer was treated as average 11 unit segments of polyindofluorene. Chromophores were assumed to localize on 4.3 units and random torsional disorder between units was assumed. The relevant disordered structures were used to calculate the electronic coupling integrals. The spectral overlap term was assumed to be constant for each chromophore while the lattice was assumed to be perfectly hexagonal. Thus, the disorder in the electronic coupling integrals was isolated. This method did not reduce an overestimated simulated L_D quite enough to match with the experimental L_D. Similarly, a constant spectral overlap term has been used for phenyl cored thiophene dendrimers. In this case, theoretical and experimental exciton diffusion lengths were found to be relatively in good agreement.[6]

4.2 Accurate Disorder

We now turn to the influence of energetic disorder on simulated L_D. Disorder in organic thin films can be simulated using the MA hopping rate (Eq. 8). This allows thermally assisted transport through an inhomogeneously broadened spectrum of exciton energies. Athanasopoulos used the MA and Förster rate equations to estimate the energy transfer rate constants with a distributed monopole INDO/CI spectral overlap term. This form of the exciton hopping rate predicts a scaling law of σ/kT,[94] where σ is the full-width-at-half-maximum of the inhomogeneously broadened spectrum. In contrast, charge carrier scaling laws go as T^{-2}.[97] This treatment has the effect of decreasing overestimated diffusion length drastically for MDMO-PPV due to increased trap concentration (Fig. 9).[95, 96] The nature of the trap sites is arbitrary, such that they may originate from chemical defects, impurities, or low energy sites. Indeed, the trap concentration for excitons in several model conjugated materials has been shown to be relatively high, on the order of 10^{18} cm^{-3}.[98, 99] The treatments described in this paragraph include the disorder in the site energies, but neglect the disorder present in the joint density of states for relaxed and unrelaxed excitons.

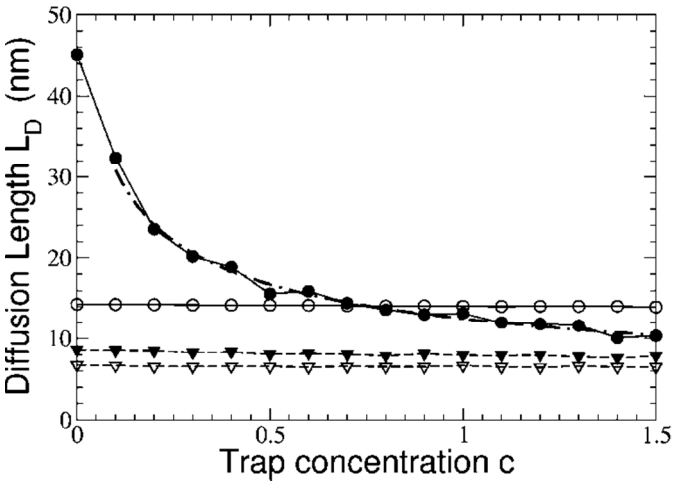

Fig. 9 Effect of trap concentration (%) on exciton diffusion length predicted with Monte-Carlo simulation in which line dipole electronic coupling integrals along with a MA/Förster type rate equation are utilized. Solid lines are at simulated at 298K, while dashed lines are simulated at 7K. Filled circles (triangles) represent inter and intrachain hopping, while empty circles (triangles) represent intrachain hopping only. Reprinted with permission from S. Athanasopoulos et al., J. Phys. Chem. C, 2008, 112, 11532-11538. Copyright 2008 American Chemical Society.[94]

Exciton diffusion simulations, which correctly account for hopping from relaxed molecular geometries, have been recently performed by Barford et al. using the concept of LEGS and

VRS with an assumed energetic disorder parameter in a Frenkel-Holstein Hamiltonian.[38] The authors rigorously include energy conservation effects in the LEGS to VRS relaxation process, i.e. dynamic localization due to vibrational relaxation. The results suggested that realistic disorder significantly decreases L_D. A similar conclusion was given by Athanasopoulos et al.[94] that torsional disorder in polymer chains considerably decreases the distance travelled by excitons.[38]

Energetic disorder and relaxation effects in the exciton energies can also be extracted from the absorption and emission spectra.[9] The energetic disorder is included in a MA type rate equation and joint density of states by assuming Gaussian broadening and classical vibrational motions.[9] However, the disorder in electronic coupling and site energies were independent. Nonetheless, molecular dynamics simulations have been able to explicitly account for correlated energetic and site coupling disorder in all parts of hopping rates for exciton diffusion.[7, 9, 100, 101]

4.3 Quantum Molecular Dynamics

There are a number of recent examples using quantum molecular dynamics simulations as input for Monte-Carlo simulations of exciton diffusion. Quantum molecular dynamics provides a correct treatment of energetic and coupling disorder and relaxation effects. An excellent methodology was pioneered by Barbosa et al., merging quantum molecular dynamics simulation with a Monte-Carlo scheme.[100] Relaxation of the molecular and electronic structures of MEH-PPV segments around an excited chromophore is executed at each time step.[100]

In contrast, a classical molecular dynamics simulation without relaxation effects (described earlier in the context of Eq. 2) was performed by Papadopoulos et al. for a liquid crystalline material.[78] Snapshots were used as input for a kinetic Monte-Carlo simulation along with INDO/CIS generated transition densities for electronic coupling calculations with TDC method. A spectral overlap term was calculated using emission and absorption data from TD-DFT calculations which were fine-tuned to include vibronic, thermal, and anharmonic effects. However, trapping due to energetic disorder was not included since each hopping rate was estimated with the same spectral overlap term.[78]

The packing and electronic structure calculations in polymer films oriented in parallel, perpendicular, and random directions with respect to a film/electrode interface were performed by Correia et al.[101] A semiempirical method similar to INDO in a quantum molecular dynamics simulation was used to produce input data for Monte-Carlo simulations. Simulated L_D was close to the experimental values. It was shown that trapping occurs predominantly in the perpendicularly aligned film. These simulations, however, did not take into account excitonic effects. The excited states were created by promotion of an electron from HOMO to LUMO without relaxation, thus relaxation effects on intramolecular disorder were not well represented. Yet, the authors accounted for energetic and site coupling disorder in the simulation code.[101]

4.4 Time-dependent Diffusion Coefficient

Thus far, all described simulations assume constant diffusion coefficient for exciton migration. A recent study went beyond this approximation by using a master equation approach to solve the time dependent diffusion coefficient with a boxcar density of states. The time dependence of the diffusion coefficient was determined from the parameters fit to the experimental photoluminescence decay of MEH-PPV films. However, the exciton diffusion was not evaluated against experimental diffusion length, but to the power conversion efficiency of a device. The simulation results did not compare well with the experimental results.[102] Nonetheless, the relevant work illustrated that an initial downhill migration process may occur for excitons, carrying time and energy dependence to the diffusion coefficient.

For small molecules based on diketopyrrolopyrrole derivatives, Li et al. predicted a general timescale for downhill migration of 10 ps. The hopping rate for these simulations was based on the nonadiabatic couplings between sites calculated with a range corrected TD-DFT functional. The nonadiabatic coupling integrals were calculated according to the Hellman-Feynman theorem.[48] The speed of relaxation was mapped out for different initial excited states and similar time dependence was found for each one (Fig. 10).[7] This relaxation process was also discussed indirectly by Westenhoff and coworkers for solvated poly[3-(2,5-dioctylphenyl)thiophene] using a Monte-Carlo approach and line dipole approximation.[103] They note slower anisotropy decay with increasing chain length. Since chain length is related to exciton energy and anisotropy decay is related to hopping rate, this study shows how a time dependent diffusion coefficient can arise as the exciton energy decreases due to hopping to lower energy sites. It is important to note that the relevant work[103] does not take into account the relaxation process inherent in the molecular Stoke's shift, while the former study[7] does.

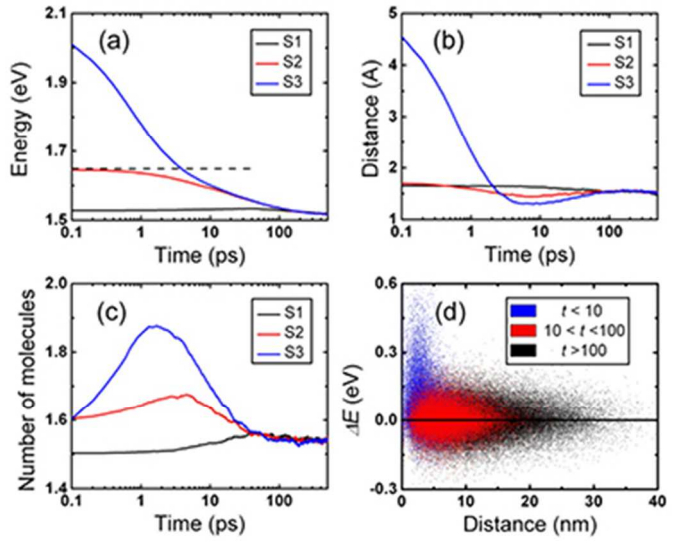

Fig. 10 Effects of initial excited state on (a) spectral migration, (b) electron-hole separation, (c) number of molecules spanned by exciton (d) change in exciton energy for the S3 exciton from Monte-Carlo simulations using transfer rates from nonadiabatic couplings calculated with TD-DFT. Reprinted with permission from Z. Li, X. Zhang and G. Lu, J. Phys.: Cond. Matt., 2014, 26, 185006. Copyright 2014 Institute of Physics.[104]

4.5 Aggregate States

The previous simulations, with the exception of Ref. 100, are performed in the context of single molecule/chain approximation, but there is evidence that multichain or multimolecule exciton energy transfer, i.e. supertransfer, can have a strong impact on the extent of exciton diffusion. Traub et al. studied single molecule excitation/emission anisotropy of polymer chains and simulated energy migration for chain morphologies generated pseudorandomly. The authors found that excitons travel 6.2 nm between excitation and emission, a lower bound for actual L_D. The comparison of experimental and simulated results by using a master equation approach suggested that low energy sites can efficiently harvest energy at long range.[105]

Support for this notion is also found in a recent study which exploited synthetic analogs of MEH-PPV in single molecule fluorescence studies. The results indicate that 'kinked' chains cause conjugation breaking. These results support a model where chains of sufficient length (>50 kDa) can fold back on themselves and form aggregate structures, which have a red-shifted absorption spectrum.[106] The excimers formed upon light absorption can perform supertransfers between aggregates[107, 108] which may result in lessening the effects of trap sites on exciton diffusion if those trap sites are the result of aggregate states. The implications and the extent of supertransfer between low energy aggregate sites is a direction for future studies.

5. Conclusions and Outlook

Exciton diffusion length simulations are important to understand the behaviour of condensed matter upon light absorption in organic matrices. Control of exciton diffusion length is essential for devices which use excitons as energy carriers. Therefore, it is vital to understand the parameters governing the magnitude of L_Ds in conjugated polymers and small molecules. Then, it will be possible to tailor the structural properties of materials for target oriented synthesis.

Both simulations and experimental findings indicate that the major contribution to L_D comes from ordered phases of thin films. However, this does not undermine the importance of exciton sizes, the strength of transition dipoles, and structural features of chromophores involved in exciton localization/delocalization. Specifically, the dependence of L_D with the variation in the building blocks of the conjugated materials has not been investigated so far. While this may present a huge challenge for the researchers in this field due to many factors affecting the extent of energy transfer in conjugated materials, a systematic and careful joint theoretical and experimental analysis might yield fruitful research results.

The vast increases in computational power that we have been enjoying in the past decades dictate us to use atomistic scale simulations for better and more accurate simulation efforts. In this regard, the excitonic coupling integrals should be estimated using highly accurate quantum mechanical approaches. The coupling between LEGS and VRS should be computed in an atomistically simulated film for generation of input data in kinetic Monte-Carlo schemes. Incorporation of energetic and spatial disorder can be handled much easier in such simulated films. For a comprehensive simulation strategy, it may be necessary to include other mechanisms such as coherent exciton transport and supertransfers.

In general, the conjugated polymers possess L_Ds ranging from 5-12 nm (omitting outliers), whereas L_Ds for small molecules can reach up to 65 nm. Such difference can be in part attributed to crystalline and densely packed nature of small molecules, which enable efficient electronic coupling of adjacent chromophores. Though, an additional factor for the relatively shorter L_D of conjugated polymers is the presence of highly concentrated traps within the films.[98] Exciton diffusion length measurements yield a number for bulk but fail to differentiate the variation in exciton migration at nanoscale. Experimental studies along with simulations can help to reveal the parameters important for exciton diffusion in organic semiconductors. Some of the recent studies in that regard have been discussed in this review. However, there is a need for extensive simulation efforts for better understanding material properties in this important class of materials.

Acknowledgements

J.A.B. acknowledges the support of the Center for Nonlinear Studies (CNLS) at Los Alamos National Laboratory (LANL) and the U.S. Department of Energy through the LANL LDRD Program. LANL is operated by Los Alamos National Security, LLC, for the National Nuclear Security Administration of the U.S. Department of Energy under contract DE-AC52-06NA25396. M.E.K acknowledges the support by TUBITAK BIDEB Fellowship.

Notes and references

[a] Center for Nonlinear Studies, Theoretical Division, Los Alamos National Laboratory, Los Alamos, NM 87545, United States. E-mail: jbjorgaard@lanl.gov.

[b] TUBITAK Gebze Yerleskesi Marmara Research Center P.O. Box 54 Gebze, Kocaeli 41470 Turkey. Phone: +90 262 679 5000 / 3711. Fax: +90 262 679 5001. *Corresponding Author. E-mail: erkan.kose@tubitak.gov.tr

1. J. L. Bredas, D. Beljonne, V. Coropceanu and J. Cornil, *Chemical Reviews*, 2004, **104**, 4971-5003.
2. G. Wei, R. R. Lunt, K. Sun, S. Wang, M. E. Thompson and S. R. Forrest, *Nano Letters*, 2010, **10**, 3555-3559.
3. R. R. Lunt, J. B. Benziger and S. R. Forrest, *Advanced Materials*, 2010, **22**, 1233-+.
4. R. J. Kline and M. D. McGehee, *Polymer Reviews*, 2006, **46**, 27-45.

5. V. Coropceanu, J. Cornil, D. A. da Silva, Y. Olivier, R. Silbey and J. L. Bredas, *Chemical Reviews*, 2007, **107**, 926-952.
6. M. E. Kose, P. Graf, N. Kopidakis, S. E. Shaheen, K. Kim and G. Rumbles, *ChemPhysChem*, 2009, **10**, 3285-3294.
7. Z. Li, X. Zhang, C. F. Woellner and G. Lu, *Applied Physics Letters*, 2014, **104**, 143303.
8. S. M. Menke and R. J. Holmes, *Energy & Environmental Science*, 2014, **7**, 499-512.
9. J. A. Bjorgaard and M. E. Kose, *Journal of Physical Chemistry C*, 2014, **118**, 5756-5761.
10. G. D. Scholes, *Annual Review of Physical Chemistry*, 2003, **54**, 57-87.
11. J. E. Kroeze, T. J. Savenije, M. J. W. Vermeulen and J. M. Warman, *Journal of Physical Chemistry B*, 2003, **107**, 7696-7705.
12. P. E. Shaw, A. Ruseckas and I. D. W. Samuel, *Advanced Materials*, 2008, **20**, 3516-+.
13. S. Cook, L. Y. Han, A. Furube and R. Katoh, *Journal of Physical Chemistry C*, 2010, **114**, 10962-10968.
14. O. V. Mikhnenko, H. Azimi, M. Scharber, M. Morana, P. W. M. Blom and M. A. Loi, *Energy & Environmental Science*, 2012, **5**, 6960-6965.
15. D. E. Markov, C. Tanase, P. W. M. Blom and J. Wildeman, *Physical Review B*, 2005, **72**, 045217.
16. A. J. Lewis, A. Ruseckas, O. P. M. Gaudin, G. R. Webster, P. L. Burn and I. D. W. Samuel, *Organic Electronics*, 2006, **7**, 452-456.
17. J. A. Bjorgaard and M. E. Kose, *Journal of Applied Physics*, 2013, **113**, 203707.
18. J. C. Bolinger, M. C. Traub, T. Adachi and P. F. Barbara, *Science*, 2011, **331**, 565-567.
19. D. E. Markov, E. Amsterdam, P. W. M. Blom, A. B. Sieval and J. C. Hummelen, *Journal of Physical Chemistry A*, 2005, **109**, 5266-5274.
20. S. R. Scully and M. D. McGehee, *Journal of Applied Physics*, 2006, **100**, 034907.
21. A. Haugeneder, M. Neges, C. Kallinger, W. Spirkl, U. Lemmer, J. Feldmann, U. Scherf, E. Harth, A. Gugel and K. Mullen, *Physical Review B*, 1999, **59**, 15346-15351.
22. A. Bruno, L. X. Reynolds, C. Dyer-Snaith, J. Nelson and S. A. Haque, *Journal of Physical Chemistry C*, 2013, **117**, 19832-19838.
23. A. Huijser, T. J. Savenije, S. C. J. Meskers, M. J. W. Vermeulen and L. D. A. Siebbeles, *Journal of the American Chemical Society*, 2008, **130**, 12496-12500.
24. D. Z. Garbuzov, V. Bulovic, P. E. Burrows and S. R. Forrest, *Chemical Physics Letters*, 1996, **249**, 433-437.
25. D. S. Qin, P. Gu, R. S. Dhar, S. G. Razavipour and D. Y. Ban, *Physica Status Solidi a-Applications and Materials Science*, 2011, **208**, 1967-1971.
26. S. Yoo, B. Domercq and B. Kippelen, *Applied Physics Letters*, 2004, **85**, 5427-5429.
27. A. K. Topczak, T. Roller, B. Engels, W. Brütting and J. Pflaum, *Physical Review B*, 2014, **89**, 201203.
28. G. D. Scholes and G. Rumbles, *Nature Materials*, 2006, **5**, 683-696.
29. W. Barford, D. G. Lidzey, D. V. Makhov and A. J. H. Meijer, *Journal of Chemical Physics*, 2010, **133**, 044504.
30. W. Barford and D. Trembath, *Physical Review B*, 2009, **80**, 165418.
31. W. J. D. Beenken, *Physica Status Solidi a-Applications and Materials Science*, 2009, **206**, 2750-2756.
32. F. C. Spano and C. Silva, *Annual Review of Physical Chemistry*, 2014, **65**, 477-500.
33. F. Paquin, H. Yamagata, N. J. Hestand, M. Sakowicz, N. Berube, M. Cote, L. X. Reynolds, S. A. Haque, N. Stingelin, F. C. Spano and C. Silva, *Physical Review B*, 2013, **88**, 155202.
34. F. C. Spano, *Journal of Chemical Physics*, 2005, **122**, 234701.
35. B. G. Sumpter, P. Kumar, A. Mehta, M. D. Barnes, W. A. Shelton and R. J. Harrison, *Journal of Physical Chemistry B*, 2005, **109**, 7671-7685.
36. J. A. Bjorgaard and M. E. Kose, *Journal of Physical Chemistry A*, 2013, **117**, 3869-3876.
37. D. V. Makhov and W. Barford, *Physical Review B*, 2010, **81**, 165201.
38. W. Barford, E. R. Bittner and A. Ward, *Journal of Physical Chemistry A*, 2012, **116**, 10319-10327.
39. W. Barford, *Journal of Physical Chemistry A*, 2013, **117**, 2665-2671.
40. J. L. Bredas and R. Silbey, *Science*, 2009, **323**, 348-349.
41. E. Collini and G. D. Scholes, *Science*, 2009, **323**, 369-373.
42. I. Hwang and G. D. Scholes, *Chemistry of Materials*, 2010, **23**, 610-620.
43. G. D. Scholes and K. P. Ghiggino, *Journal of Physical Chemistry*, 1994, **98**, 4580-4590.
44. D. Beljonne, G. Pourtois, C. Silva, E. Hennebicq, L. M. Herz, R. H. Friend, G. D. Scholes, S. Setayesh, K. Mullen and J. L. Bredas, *Proceedings of the National Academy of Sciences of the United States of America*, 2002, **99**, 10982-10987.
45. E. Hennebicq, G. Pourtois, G. D. Scholes, L. M. Herz, D. M. Russell, C. Silva, S. Setayesh, A. C. Grimsdale, K. Mullen, J. L. Bredas and D. Beljonne, *Journal of the American Chemical Society*, 2005, **127**, 4744-4762.
46. K. Brunner, A. Tortschanoff, C. Warmuth, H. Bassler and H. F. Kauffmann, *Journal of Physical Chemistry B*, 2000, **104**, 3781-3790.
47. J. Clark, T. Nelson, S. Tretiak, G. Cirmi and G. Lanzani, *Nature Physics*, 2012, **8**, 225-231.
48. K. Gottfried, *Quantum Mechanics: Fundamentals Second Edition*, Springer, New York, 2004.
49. V. May and O. Kühn, *Charge and energy transfer dynamics in molecular systems*, John Wiley & Sons, 2008.
50. M. E. Kose, *Journal of Chemical Physics*, 2011, **135**, 244512.
51. M. E. Kose, *Journal of Physical Chemistry C*, 2011, **115**, 13076-13082.
52. W. J. D. Beenken and T. Pullerits, *Journal of Chemical Physics*, 2004, **120**, 2490-2495.
53. S. E. Koh, C. Risko, D. A. da Silva, O. Kwon, A. Facchetti, J. L. Bredas, T. J. Marks and M. A. Ratner, *Advanced Functional Materials*, 2008, **18**, 332-340.
54. M. Kasha, *Radiation Research*, 1963, **20**, 55-&.
55. R. D. Harcourt, G. D. Scholes and K. P. Ghiggino, *Journal of Chemical Physics*, 1994, **101**, 10521-10525.
56. G. D. Scholes, R. D. Harcourt and K. P. Ghiggino, *Journal of Chemical Physics*, 1995, **102**, 9574-9581.
57. J. Neugebauer, *Journal of Chemical Physics*, 2007, **126**, 134116.

58. C. Koonig, N. Schluuter and J. Neugebauer, *Journal of Chemical Physics*, 2013, **138**, 034104.
59. B. P. Krueger, G. D. Scholes and G. R. Fleming, *Journal of Physical Chemistry B*, 1998, **102**, 5378-5386.
60. M. E. Kose, W. J. Mitchell, N. Kopidakis, C. H. Chang, S. E. Shaheen, K. Kim and G. Rumbles, *J. Am. Chem. Soc.*, 2007, **129**, 14257-14270.
61. A. Dreuw and M. Head-Gordon, *Chemical Reviews*, 2005, **105**, 4009-4037.
62. L. Genovese, T. Deutsch, A. Neelov, S. Goedecker and G. Beylkin, *Journal of Chemical Physics*, 2006, **125**, 074105.
63. A. Czader and E. R. Bittner, *Journal of Chemical Physics*, 2008, **128**, 035101.
64. T. Forster, *Annalen Der Physik*, 1948, **2**, 55-75.
65. T. Forster, *Discussions of the Faraday Society*, 1959, 7-17.
66. M. M. L. Grage, Y. Zaushitsyn, A. Yartsev, M. Chachisvilis, V. Sundstrom and T. Pullerits, *Physical Review B*, 2003, **67**, 205207.
67. M. M. L. Grage, P. W. Wood, A. Ruseckas, T. Pullerits, W. Mitchell, P. L. Burn, I. D. W. Samuel and V. Sundstrom, *Journal of Chemical Physics*, 2003, **118**, 7644-7650.
68. S. Westenhoff, C. Daniel, R. H. Friend, C. Silva, V. Sundstrom and A. Yartsev, *Journal of Chemical Physics*, 2005, **122**, 094903.
69. B. Movaghar, M. Grunewald, B. Ries, H. Bassler and D. Wurtz, *Physical Review B*, 1986, **33**, 5545-5554.
70. B. Movaghar and W. Schirmacher, *Journal of Physics C-Solid State Physics*, 1981, **14**, 859-880.
71. L. Pautmeier, B. Ries, R. Richert and H. Bassler, *Chemical Physics Letters*, 1988, **143**, 459-462.
72. R. Richert, B. Ries and H. Bassler, *Philosophical Magazine B-Physics of Condensed Matter Statistical Mechanics Electronic Optical and Magnetic Properties*, 1984, **49**, L25-L30.
73. S. Rughooputh, D. Bloor, D. Phillips and B. Movaghar, *Physical Review B*, 1987, **35**, 8103-8112.
74. G. Vaubel and H. Baessler, *Molecular Crystals and Liquid Crystals*, 1970, **12**, 47-&.
75. C. Madigan and V. Bulovic, *Physical Review Letters*, 2006, **96**, 046404.
76. V. Stehr, R. F. Fink, B. Engels, J. Pflaum and C. Deibel, *Journal of Chemical Theory and Computation*, 2014, **10**, 1242-1255.
77. S. T. Hoffmann, H. Bassler and A. Kohler, *Journal of Physical Chemistry B*, 2010, **114**, 17037-17048.
78. T. A. Papadopoulos, L. Muccioli, S. Athanasopoulos, A. B. Walker, C. Zannoni and D. Beljonne, *Chemical Science*, 2011, **2**, 1025-1032.
79. F. C. Spano, *Chemical Physics*, 2006, **325**, 22-35.
80. F. C. Spano, in *Annual Review of Physical Chemistry*, 2006, vol. 57, pp. 217-243.
81. F. C. Spano, J. Clark, C. Silva and R. H. Friend, *Journal of Chemical Physics*, 2009, **130**, 074904.
82. O. R. Tozer and W. Barford, *Journal of Physical Chemistry A*, 2012, **116**, 10310-10318.
83. W. Barford and O. R. Tozer, *Journal of Chemical Physics*, 2014, **141**, 164103.
84. M. Casalegno, G. Raos and R. Po, *Journal of Chemical Physics*, 2010, **132**, 094705.
85. A. F. Voter, *INTRODUCTION TO THE KINETIC MONTE CARLO METHOD*, 2007.
86. T. K. Mullenbach, K. A. McGarry, W. A. Luhman, C. J. Douglas and R. J. Holmes, *Advanced Materials*, 2013, **25**, 3689-3693.
87. M. Brinkmann, *Journal of Polymer Science Part B-Polymer Physics*, 2011, **49**, 1218-1233.
88. M. Brinkmann and P. Rannou, *Macromolecules*, 2009, **42**, 1125-1130.
89. Y. Tamai, Y. Matsuura, H. Ohkita, H. Benten and S. Ito, *The Journal of Physical Chemistry Letters*, 2014, **5**, 399-403.
90. M. Sim, J. Shin, C. Shim, M. Kim, S. B. Jo, J. H. Kim and K. Cho, *Journal of Physical Chemistry C*, 2014, **118**, 760-766.
91. V. Ern, *Physical Review Letters*, 1969, **22**, 343-&.
92. V. Stehr, B. Engels, C. Deibel and R. F. Fink, *Journal of Chemical Physics*, 2014, **140**, 024503.
93. Z. Masri, A. Ruseckas, E. V. Emelianova, L. J. Wang, A. K. Bansal, A. Matheson, H. T. Lemke, M. M. Nielsen, H. Nguyen, O. Coulembier, P. Dubois, D. Beljonne and I. D. W. Samuel, *Advanced Energy Materials*, 2013, **3**, 1445-1453.
94. S. Athanasopoulos, E. V. Emelianova, A. B. Walker and D. Beljonne, *Physical Review B*, 2009, **80**, 195209.
95. S. Athanasopoulos, E. V. Emelianova, A. B. Walker and D. Beljonne, in *Organic Photonics Iv*, eds. P. L. Heremans, R. Coehoorn and C. Adachi, 2010, vol. 7722.
96. S. Athanasopoulos, E. Hennebicq, D. Beljonne and A. B. Walker, *Journal of Physical Chemistry C*, 2008, **112**, 11532-11538.
97. V. I. Arkhipov, J. Reynaert, Y. D. Jin, P. Heremans, E. V. Emelianova, G. J. Adriaenssens and H. Bassler, *Synthetic Metals*, 2003, **138**, 209-212.
98. O. V. Mikhnenko, M. Kuik, J. Lin, N. van der Kaap, T. Q. Nguyen and P. W. M. Blom, *Advanced Materials*, 2014, **26**, 1912-1917.
99. Z. Q. Liang and B. A. Gregg, *Advanced Materials*, 2012, **24**, 3258-3262.
100. H. M. C. Barbosa, H. M. G. Correia and M. M. D. Ramos, *Journal of Nanoscience and Nanotechnology*, 2010, **10**, 1148-1152.
101. H. M. G. Correia, H. M. C. Barbosa, L. Marques and M. M. D. Ramos, *Computational Materials Science*, 2013, **75**, 18-23.
102. V. M. Burlakov, K. Kawata, H. E. Assender, G. A. D. Briggs, A. Ruseckas and I. D. W. Samuel, *Physical Review B*, 2005, **72**, 075206.
103. S. Westenhoff, W. J. D. Beenken, A. Yartsev and N. C. Greenham, *Journal of Chemical Physics*, 2006, **125**, 154903.
104. Z. Li, X. Zhang and G. Lu, *Journal of Physics-Condensed Matter*, 2014, **26**, 185006.
105. M. C. Traub, G. Lakhwani, J. C. Bolinger, D. Vanden Bout and P. F. Barbara, *Journal of Physical Chemistry B*, 2011, **115**, 9941-9947.
106. M. C. Traub, J. Vogelsang, K. N. Plunkett, C. Nuckolls, P. F. Barbara and D. A. Vanden Bout, *ACS Nano*, 2012, **6**, 523-529.
107. D. J. Heijs, V. A. Malyshev and J. Knoester, *Physical Review Letters*, 2005, **95**, 177402.
108. G. D. Scholes, *Chemical Physics*, 2002, **275**, 373-386.

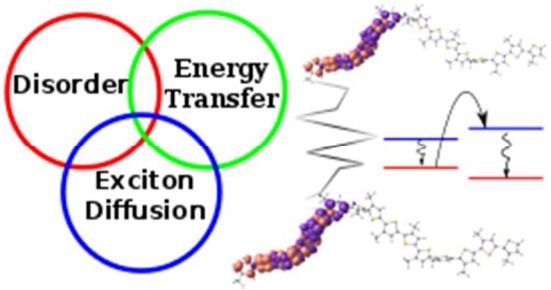

Recent advances in exciton diffusion simulations in conjugated materials are presented in this review.
100x50mm (72 x 72 DPI)